Design of Mechanism-Based Inhibitors of Transthyretin Amyloidosis: Studies with Biphenyl Ethers and New Structural Templates

Sarika Gupta,[†,§] Manmohan Chhibber,[‡,§] Sharmistha Sinha,[‡] and Avadhesha Surolia*,[†]

Molecular Biophysics Unit, Indian Institute of Sciences, Bangalore 560012, India, and National Institute of Immunology, Aruna Asaf Ali Marg, New Delhi 110067, India

Transthyretin (TTR), a tetrameric thyroxine (T4) carrier protein, is associated with a variety of amyloid diseases. In this study, we explore the potential of biphenyl ethers (BPE), which are shown to interact with a high affinity to its T4 binding site thereby preventing its aggregation and fibrillogenesis. They prevent fibrillogenesis by stabilizing the tetrameric ground state of transthyretin. Additionally, we identify two new structural templates (2-(5-mercapto-[1,3,4]oxadiazol-2-yl)-phenol and 2,3,6-trichloro-*N*-(4*H*-[1,2,4]triazol-3-yl) represented as compounds **11** and **12**, respectively, throughout the manuscript) exhibiting the ability to arrest TTR amyloidosis. The dissociation constants for the binding of BPEs and compound **11** and **12** to TTR correlate with their efficacies of inhibiting amyloidosis. They also have the ability to inhibit the elongation of intermediate fibrils as well as show nearly complete (>90%) disruption of the preformed fibrils. The present study thus establishes biphenyl ethers and compounds **11** and **12** as very potent inhibitors of TTR fibrillization and inducible cytotoxicity.

Introduction

Protein misfolding, misassembly, and extracellular deposition are related to a class of diseases collectively known as "conformational diseases", which include Alzheimer's disease,[1] prion disease,[2] dialysis-related amyloidosis,[3] familial amyloid polyneuropathy,[4] and type II diabetes.[5] Most of these diseases are incurable and fatal. The proteins and peptides related to these diseases can self-assemble into supramolecular assemblies with a common cross-β structure. Despite a large variation in their sequences and native structures, they adopt a similar morphology upon fibril formation, which suggests that there is a common mechanism underlying amyloid fibril formation.[6]

Transthyretin (TTR[a]), a tetrameric protein, transports thyroxine and *holo* retinol binding protein in plasma and cerebrospinal fluid.[7] Further, it also scavenges Aβ peptide, preventing its aggregation and thereby regulates the pathogenesis of Alzheimer's disease.[8] TTR tetramer has a tendency to dissociate to unfolded monomers, which aggregate together resulting in the formation of amyloid fibers, which constitute the hallmark of familial amyloid cardiomyopathy (FAC), senile systemic amyloidosis (SSA, late onset), and familial amyloid polyneuropathy (FAP, early onset). In SSA and FAC, wild type TTR forms amyloid deposits on the cardiac and other tissues.[9,10] Approximately 100 mutants have been identified in TTR to be involved in FAP, which affect the peripheral and autonomic nervous system, heart,[8] and the CNS.[11,12] Irrespective of the types of TTR (viz. wild type TTR or its mutants) involved in amyloid formation, the overall mechanism of fibril formation is similar. The common mechanism involves the dissociation of the tetramer into non-native monomers, which eventually

agglomerate into fibers.[12] TTR deposits are predominantly extracellular in nature, while some of its variants also exhibit tissue specificity.[14] The mechanism for their tissue selectivity and the pathway of their deposition *in vivo* are as yet poorly understood.

The quaternary structure of TTR contains two funnel shaped thyroxine (T4) binding sites.[15] Under physiological conditions, only 10−25% of T4 in the plasma is bound to TTR.[16] The stabilization of TTR tetramer by small molecules, which bind to the T4 pocket, is an emerging theme in a number of studies aiming to stall amyloidogenic potential of TTR.[17,18] So far, a number of TTR amyloidosis inhibitors including both natural and synthetic molecules that span a variety of structural classes have met with limited success.[19−38] Chemical modification and covalent linking of molecules to TTR have also been suggested as alternatives to these approaches.[39−41]

Biphenyl ether as a template to design potential inhibitors of TTR amyloidosis has not yet been explored systematically. The structure−activity relationship (SAR) studies have shown that small molecule such as triclosan, could inhibit TTR aggregation.[42] Triclosan, which has a biphenyl ether skeleton, resembles T4 in its gross structure (Figure 1a). Triclosan exhibits a wide range of pharmacological properties including antibacterial and antimalarial activities.[43] In the present report, we have synthesized a series of BPE derivatives (Figure 1b and Table 1) and investigated their ability to arrest TTR amyloidosis using a variety of biochemical and biophysical methods. We also report their striking ability to disrupt preformed fibers and restore the native tetrameric state of TTR. We also report results from screening of a library of 100 compounds to obtain some new scaffolds for inhibiting amyloidosis. Docking studies were performed to provide a rationale for the inhibitory potencies of BPEs in preventing TTR amyloidosis.

Results

Fibril Formation Assay. The stagnant fibril formation assay at pH 4.4 showed that all the synthetic BPEs examined inhibited TTR amyloidosis at stoichiometric concentration (Table S2 in Supporting Information). Out of 24 designed BPEs, nine

---

* Author to whom correspondence should be addressed. Fax: +91-11-26162125, e-mail: surolia@nii.res.in.
‡ Indian Institute of Sciences.
† National Institute of Immunology.
§ These authors have made equal contributions.

[a] Abbreviations: TTR, transthyretin; BPEs, biphenyl ethers; T4, thyroxine; SAR, structure−activity relationship; MALDI-TOF, matrix-assisted laser desorption ionization-time of flight; Th-T, thioflavin-T; TEM, transmission electron microscope.
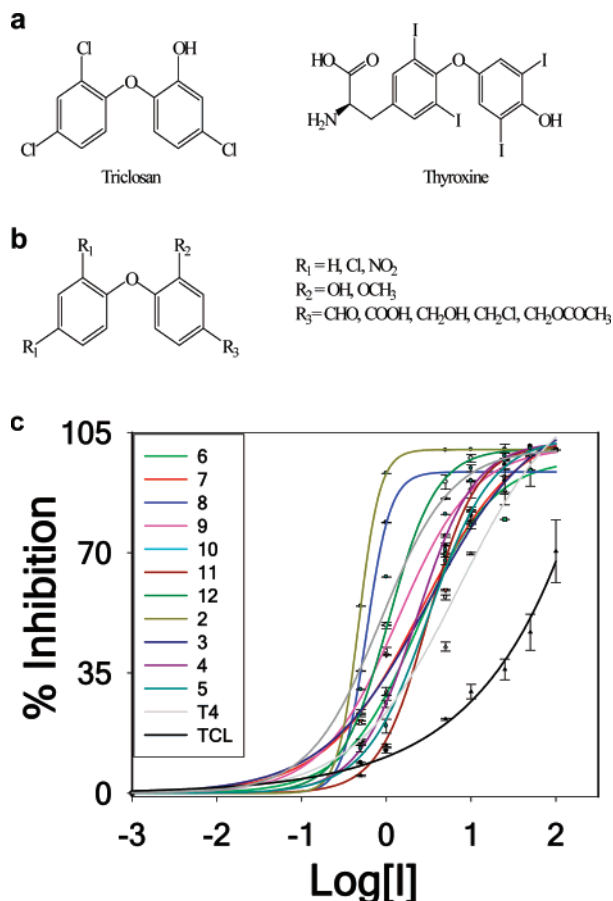
Figure 1. (a) Structures of triclosan and thyroxine, (b) Strategy for the design of differently substituted BPE derivatives. (c) The semilog plot of TTR (7.2 μM) stagnant acid-mediated fibrillization assay at pH 4.4 in the presence of compounds **1**–**12** and thyroxine at various concentrations over 72 h. The experiment was performed at 37 °C. The data were fitted in to sigmoid equation as given in Supporting Information, and the IC$_{50}$ value was calculated graphically. Results are the mean of five independent experiments with error bar.

compounds (represented as **2**–**10** in Table 1) inhibited the process >90% when 3 molar equiv of them were used over TTR (BPEs = 21.6 μM, TTR = 7.2 μM), except triclosan (~24%), and were therefore selected for a detailed study. BPEs were found more effective as inhibitors than T4.

Out of the 100 compounds from the chemical library, 41 compounds were found to inhibit fibril formation at 100 μM concentrations (Table S1 in Supporting Information). Of these, only two compounds **11** and **12** were selected for further studies, as they inhibited TTR (7.2 μM) fibrillization completely at 21.6 μM (Table 1). IC$_{50}$ for compounds **2**–**12** are in the range of 0.47–3.5 μM, which are lower than IC$_{50}$ of 7.1 μM for its natural ligand T4 (Table 1). The dose-dependent curves for inhibition of TTR amyloid formation by these compounds are shown in Figure 1c. The dissociation constant K_{d1} of compounds **2**–**12** at pH 4.4, are in nanomolar range compared to 144.0 μM of triclosan (Table 1). For compounds **2**, **3**, **4**, **6**, and **10**, the K_{d2} is 37–10000-fold higher than their respective K_{d1}, suggesting negative cooperativity for their binding to the second site of TTR.

Compounds buffered at pH 4.4 have also acted as potent inhibitors of the process. Table 1 shows the stoichiometry of binding of the compounds **1**–**12** to TTR tetramer. Further, in order to rule out the presence of any fibrillar species, inhibition of fibril formation by compounds **1**–**12** was tested by Congo red binding. A comparison of the results of turbidity assay at

340 nm and of quantitative Congo red binding to fibril formed by TTR in the presence and absence of inhibitors is shown in Figure 2a. While unligated TTR exhibited maximum binding of Congo red, it was significantly reduced in the presence of compounds **1**–**12**. Even 7–30 days old samples in the presence of compounds **1**–**12** exhibited diminished binding of Congo red to TTR. TTR fibrillization in the presence and absence of compounds **1**–**12** was further examined by TEM. As is evident from TEM pictures (Figure S1; see Supporting Information) the samples containing compounds **2**–**12** were devoid of any fiber or amorphous aggregates. In contrast, BPE-untreated samples exhibit fiber and fibrillar aggregates in abundance.
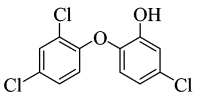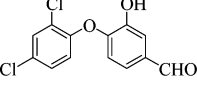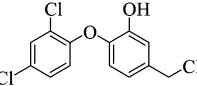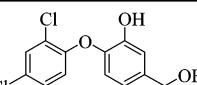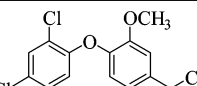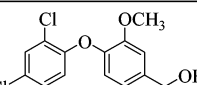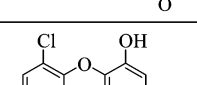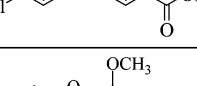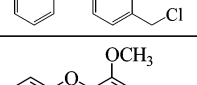
Kinetics of Fibril Formation. The kinetics of fibril formation in the presence and absence of the compounds were monitored by linear increase in the turbidity at 340 nm for 3 h. The increase is prominent in the absence of inhibitors, while it was significantly reduced in the presence of the inhibitors and T4. The inhibition was >80% by compounds **2**–**12** and 62% by triclosan as compared to 75% inhibition by T4 (Figure 2b). These results are consistent with the results of stagnant fibril formation assay (Figure 2a). The rate of fibril formation in the presence and absence of compounds **1**–**12** is given in Figure S2 (see Supporting Information).

Thioflavin-T (Th-T) Fluorescence. Th-T fluorescence was monitored in the presence and absence of the inhibitors at pH 4.4 at 0 and 72 h. The intensity of Th-T was high in the absence of the compounds **2**–**12** and significantly less in their presence (Figure 2c). There was no significant increase in Th-T binding even in the samples incubated for 7–30 days in the presence of compounds **1**–**12** (data not shown).
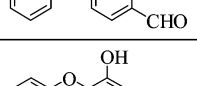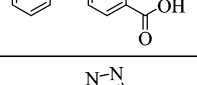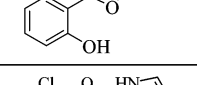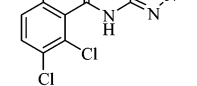
Tryptophan Fluorescence. TTR exhibits fluorescence emission maxima at 339 and 343 nm, respectively, at pH 7.2 and 4.4, indicating the presence of tryptophan residues exposed to solvent at the surface of the protein. Conformational changes in TTR induced upon binding of inhibitors therefore were studied by monitoring the intrinsic fluorescence of the protein in the presence and absence of the compounds **2**–**12**, triclosan, and T4 both at pH 7.2 and 4.4. A significant reduction in the fluorescence intensity of TTR was observed in the presence of compounds **1**–**4** and **6**–**12** at pH 7.2 (Figure 3a), which was more pronounced at pH 4.4 (Figure 3b). This indicates a subtle change in the exposure of tryptophan residue(s) in TTR upon the binding of compounds **1**–**12**, which in turn appears to be a reflection of a change of its quaternary structure. A comparison of the change in fluorescence intensity of TTR treated with the compounds **1**–**12** show a greater reduction at pH 4.4 as compared to that at pH 7.2, indicating that at acidic pH a greater proportion of TTR is being driven to tetramer formation by the binding of these compounds.

Urea Denaturation. As the rate of TTR fibrillization is proportional to the rate of tetramer dissociation, the rate and extent of TTR tetramer (1.8 μM) dissociation in 6.0 M urea was monitored by evaluating the intrinsic fluorescence of TTR. Compounds **1**–**12** exert substantial effect on the amplitude of TTR tetramer dissociation (Figure 3c). For example at 1:3 ratio of TTR to triclosan, 47% of the protein dissociates as compared to the untreated control under identical conditions. In comparison, compound **7** and T4-treated TTR under similar situation exhibits 21 and 27% dissociation, respectively. Interestingly, in the presence of compounds **2**–**6** and **8**–**12**, less than 5% of the protein dissociates and unfolds even after 144 h, implying an overwhelming stabilization of TTR tetramer by these compounds (Figure 3c). These data thus allow us to infer that these compounds act by kinetic stabilization of TTR tetramer under

Table 1. Potencies of Biphenyl Ethers and Other New Structural Templates as TTR Amyloidosis Inhibitors[a]

S.N.	Compounds	%FF		IC$_{50}$ ± SE (μM)	Dissociation Constant (nM)		Stoichio-metry	Calculated energy
		1:1	1:3		K$_{d1}$	K$_{d2}$		
1	(structure)	75	66	53.5 ± 7.01	144000±5000	190.00	1:3.1	−3.225
2	(structure)	0	0	0.52 ± 0.01	13.9 ± 5.01	525.0±60.10	1:1	−3.822
3	(structure)	5	0	0.85 ± 0.08	5.7 ±1.21	1000 ±189	1:1	−3.0592
4	(structure)	12	2.6	1.36 ± 0.05	0.3 ± 0.14	13800 ±1021	1:1	−3.722
5	(structure)	26	0	3.16 ± 0.04	ND		1:2	−3.567
6	(structure)	10	0	0.475 ± 0.03	0.2± 0.08	8300±100	1:1	−3.945
7	(structure)	29	13.3	2.59 ± 0.14	27.0 ± 8.03	3.0 ± 0.78	1:2	−2.723
8	(structure)	25	0	1.94 ± 0.09	ND		1:1	ND
9	(structure)	12	0	1.31 ± 0.08	88.0± 10.06	*	1:1	−3.224
10	(structure)	32	5	3.18 ± 0.16	27± 4.10	292.0± 2.81	1:2.4	−2.964
11	(structure)	21	0	3.1 ± 0.05	42± 2.35	72.6 ± 10.32	1:2.4	−3.1564
12	(structure)	11	3.6	1.06 ± 0.01	120.0± 32.11	*	1:3.7	−3.192
13	(structure)	48	7	7.17 ± 0.21	ND		ND	ND

[a] %FF: The percent fibril formation of TTR (7.2 μM). The inhibition was tested at TTR to inhibitor ratio of 1:1 and 1:3 which corresponds to 7.2 μM and 21.6 μM inhibitor concentrations, respectively, at pH 4.4, 37 °C. Fibril formation by TTR in the absence of inhibitors was considered as 100%. IC$_{50}$ value, i.e., inhibitor concentration at which there is 50% reduction in fibril formation. Stoichiometry, the number of equivalents of inhibitor bound to one equivalent of TTR. Results presented are mean of five different experiments. ND, not determined; *, data fitted well to a single binding site.

denaturing conditions over the amyloidogenic monomer, a finding consistent with the rate of fibril formation at 37 °C, pH 4.4 (Figure 2a).

Glutaraldehyde Cross-Linking. To understand the mechanism of inhibition of fibril formation by all the above compounds, the quaternary structure of TTR in the presence and absence of these compounds at acidic condition was characterized by glutaraldehyde cross-linking followed by the analysis of the cross-linked products by SDS-PAGE. TTR at pH 7.2 migrated predominantly as a tetramer (55 kDa), whereas at pH
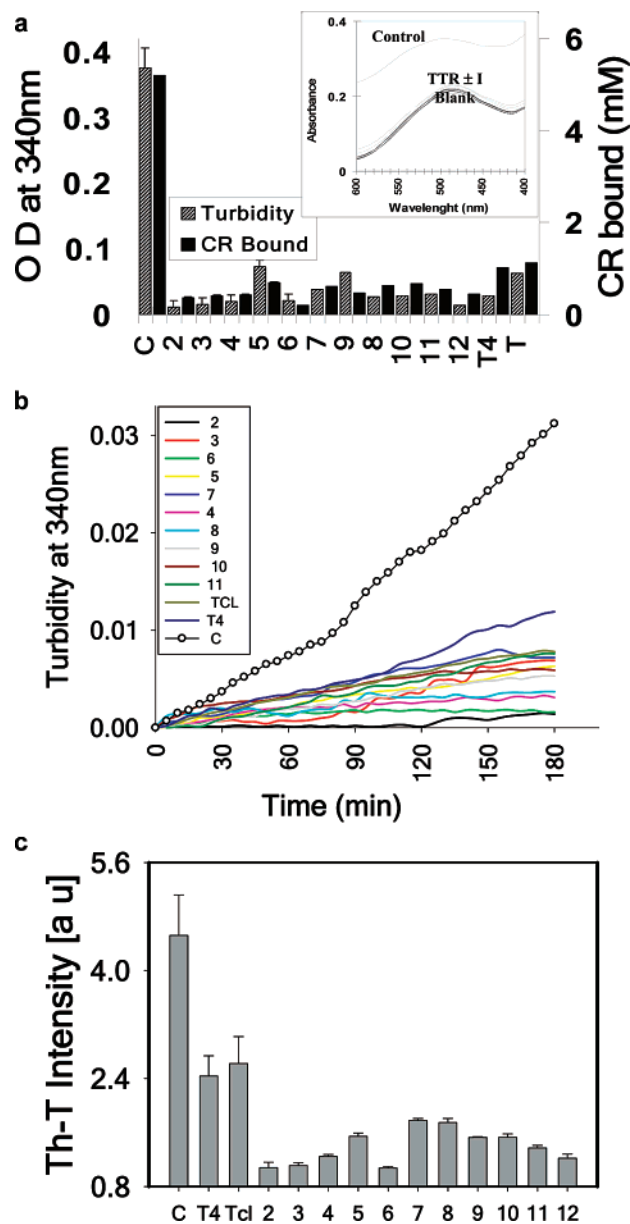
Figure 2. (a) Comparative bar diagram of turbidity (shaded bars) and quantitative Congo red binding (black bars) assay to quantitate TTR (7.2 μM) fibrillogenesis in the absence and presence of 3 equiv (21.6 μM) of compounds **1**−**12** and T4. Results are means of 3−5 different observations. Congo red binding to the TTR in the presence and absence of inhibitors after 15 days of incubation at pH 4.4 was monitored by scanning for absorption from 400−600 nm (spectra in the inset). Experiments were carried out at 37 °C. (b) The time course of TTR (7.2 μM) fibril formation in the presence and absence of compounds **1**−**12** and T4 (21.6 μM) at 37 °C, pH 4.4. Turbidity at 340 nm was monitored for 3 h is plotted against time. Results are mean of three different experiments done in triplicate. Standard error was <10%. The plot shows the rate of fibril formation in the presence and absence of compounds **1**−**12** and T4 in preventing TTR fibril formation is given in Supporting Information (Figure S2). (c) Thioflavin-T fluorescence after binding to TTR (7.2 μM) in the presence and absence of compounds **1**−**12** and T4 (21.6 μM) under fibrillization condition. Fibrils were produced by acidification at pH 4.4 for 72 h at 37 °C and monitored by the Th-T fluorescence assay. The samples were incubated with 50 μM of Th-T for 15 min at 37 °C and excited at 450 nm, and Th-T fluorescence emissions were monitored at 480 nm. Results are means of three independent experiments done in duplicate.

4.4 it migrated as a monomer (Figure 4a). However, TTR migrates predominantly as a tetramer in the presence of
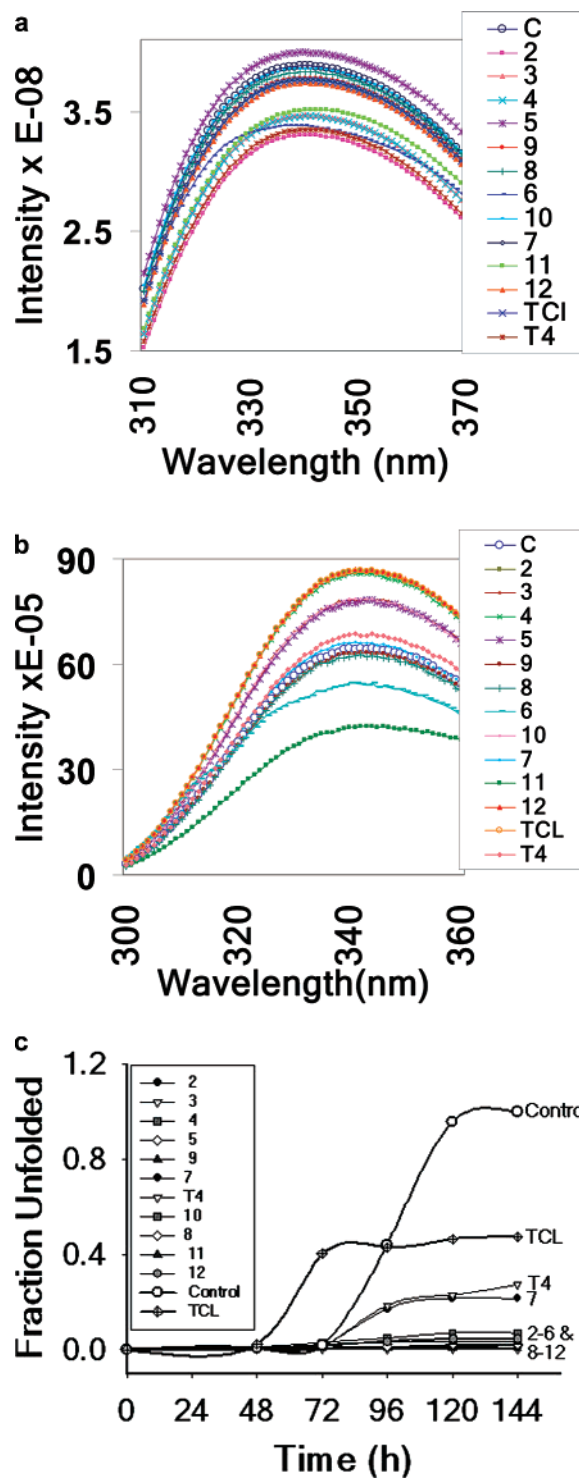
Figure 3. Conformational change in TTR induced by binding of compounds **1**−**12** and T4. TTR (3.6 μM) incubated in the presence and absence of compounds **1**−**12** (7.2 μM) at 25 °C (a) at pH 7.2, (b) at pH 4.4. Change in conformation was inferred by monitoring the intrinsic fluorescence of TTR. Samples were excited at 290 nm, and emission was monitored in the range of 310−370 nm. Results are mean of three different experiments. (c) Time dependence of tetramer dissociation (fraction unfolded) of TTR in the presence and absence of inhibitors in 6 M urea at 25 °C. TTR (1.8 μM) incubated for 1 h with 5.4 μM of compounds **1**−**12** or T4 at 25 °C at pH 7.2 was used for these studies. Urea was then added to these solutions to a final concentration of 6 M, and the unfolding of TTR was monitored by following the intrinsic fluorescence of the protein at 339 nm up to 144 h. Samples were excited at 290 nm. Fraction unfolded at each time point was plotted against time. Results are mean of three different experiments performed in duplicate.

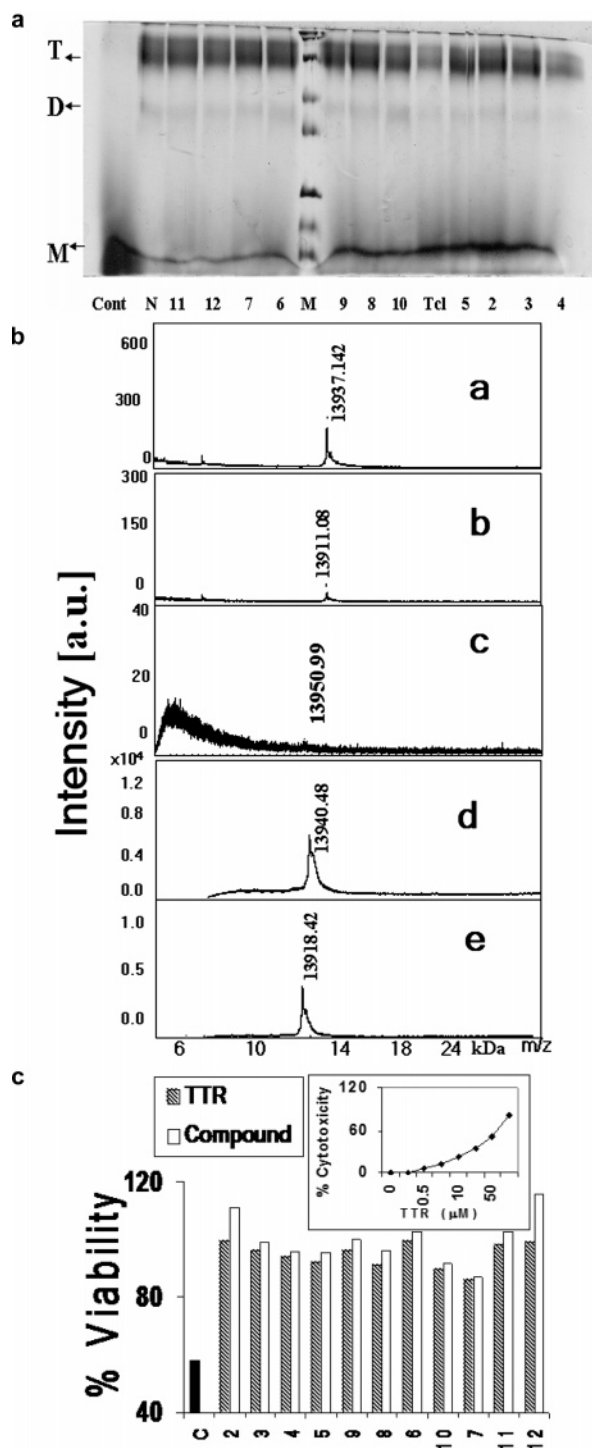**Figure 4.** a: Oligomeric status of TTR in the presence and absence of compounds **1**−**12** at pH 4.4 after 15 days of incubation under fibrillization conditions. The reaction mixtures were neutralized and the samples cross-linked with gluteraldehyde. They were then elecrophoresed on 12% SDS-PAGE. TTR complexes with compounds **1**−**12** migrated mainly as the tetramer. N, is TTR at −20 °C; M, molecular wt standards. b: Stability of TTR treated with compounds **1**−**12**. Mass spectra of TTR at (a) 0 h, (b) 72 h, (c) 7 days at pH 4.4, (d) native TTR, and (e) in presence of inhibitor 2 after 7 days. The mass spectra of TTR with compounds **3**−**12** at 15 days are given in Figure S3 in Supporting Information. c: Efficacies of compounds **2**−**12** in protecting Neuro2a cells against cytotoxicity of TTR. The graph shows the % viability of cells treated with TTR (25 μM) alone (black bar), at 2 equiv of compound **2**−**12** (50 μM) with respect to TTR concentration (hatched bars), and compounds alone (open bars). Dose-dependent curve of TTR-induced cytotoxicity to Neuro2a cells is given in the inset. Results are mean of three different experiments conducted in triplicate.

compounds **1**−**12**. Only a small amount of dimer was observed in case of native TTR and TTR in the presence of compounds **1**−**12**. In the absence of these inhibitors, the amount of tetramer was decreased with time and became zero after 3 days (data not shown). In contrast, there was no significant difference in the tetramer concentration in the presence of these inhibitors during 72 h to 30 days.

Mass Spectrometry. All the above observations clearly show that compounds **1**−**12** prevent fibril formation by stabilizing TTR tetramer. It can, therefore, be assumed that soluble TTR present in the reaction mixture mostly exists as a tetramer. To confirm these findings, MALDI-TOF of TTR samples treated with these inhibitors for 3, 7, and 15 days subsequent to centrifugation and filtration through 80 kDa cutoff membranes was carried out as described in the Experimental Section. As shown in Figure 4b, the intensity of the monomer peak gradually decreases which completely disappear by day 7 in the absence of the inhibitors (Figure 4b, a−c). In contrast, a peak corresponding to ~13850 Da can be observed in the presence of inhibitor 2, shown here as a representative example, even after 15−30 days of fibrillogenesis (Figure 4b, d and e). The mass spectra of TTR in the presence and absence of the other compounds (viz. **1** and **3**−**12**) are shown in Figure S3 (Supporting Information).

Inhibition of TTR-Induced Cell Cytotoxicity by Compounds 2−12. Neuro2A cell culture was used to detect the presence of any soluble toxic aggregates in the reaction mixture used for studying the inhibition of TTR fibrillogenesis. Preliminary experiments showed that mature TTR amyloid fibers are not cytotoxic (data not shown). However, TTR solution left under the conditions of fibrillogenesis induces toxicity to Neuro2A cells in a concentration-dependent manner in 72 h (Figure 4c). Figure 4c shows the TTR-induced ~41% cytotoxicity under the fibrillogenesis conditions. However, preincubation of TTR (25 μM) with the compounds **2**−**12** (50 μM) exhibited viability in the range of 86−99.5%. Compounds **2**−**12** at 50 μM by themselves had no effect on the survival of Neuro2A cells in culture, demonstrating their nontoxic nature at the concentrations used (Figure 4c).

Molecular Docking. To validate and understand the basis of the inhibitory activities of these closely related BPEs in TTR amyloidosis, docking studies were performed. The crystallographic structure of the TTR−T4 complex[44] showed its hormone-binding sites, which are composed of three symmetry-related hydrophobic small depressions, termed halogen-binding pockets. The molecular docking of all these inhibitors with TTR shows their binding to the T4 binding site with binding of one ring to P3 and the other to P1 pocket. Interactions with the residues lining the pocket are mainly through hydrophobic and electrostatic interactions. Figure 5 shows the overlap of several of the MOE-docked BPEs and compound **11** and **12** in the thyroxine binding pocket of TTR complexed with T4. Triclosan and other biphenyl ethers with $R_1 = Cl$ bind deep in the P3 pocket of TTR while the dihalogenated phenyl ring is positioned in the outer P1 pocket of the binding cavity, viz. the two chlorine atoms of the B-ring of tricolsan are accommodated in P1 and P1′ pockets, respectively (Figure 5). Van der Waals interactions between both the chloride substituent of the ligand and the side chains of Leu17, Ala108, Thr119, and Val121 from the adjacent TTR subunit contribute to the stabilization of the tetramer. The atoms of BPEs that are involved in extensive hydrophobic interactions with Ala108, Leu110, Ser117, Thr118, and Thr119 of the monomer AA′ and CC′ appear to contribute significantly to the overall stability of the tetrameric structure. Thus two
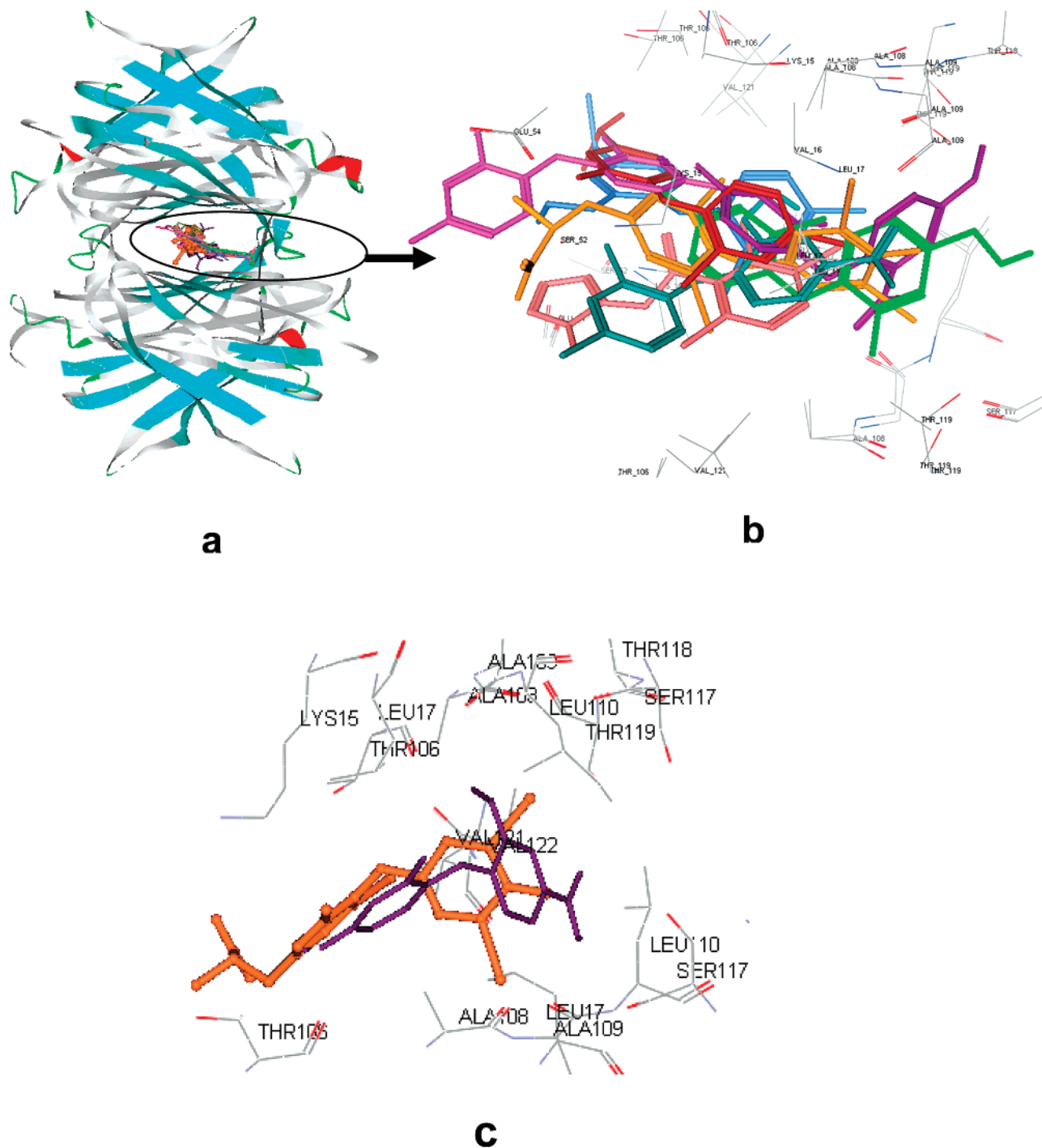
Figure 5. Results of the docking of compounds **2−12** on the TTR tetramer. Molecular docking with the TTR tetramer was done with each of the inhibitors using MOE-2005 software. There are two symmetrically equivalent positions for ligands in each tetramer of TTR. For the sake of clarity, only one of the symmetry equivalent positions of the binding site for the T4 together with other inhibitors docked therein is shown. (a) The overlap structure of docked compounds **2−12** to TTR and thyroxine (orange) bound to TTR (PDB code 2ROX). (b) Blown up version of the thyroxine binding site along with compounds **2−6**, **10**, and **12** overlapped with T4. Color codes are T4 (orange), **2** (cyan), **3** (red), **4** (light green), **5** (blue), **6** (purple), **10** (pink), and **12** (peach). (c) Overlap of the mode of binding of the best inhibitor (compound **6**; shown in purple) with T4 (orange) at the T4 binding site of TTR. The interactions between TTR and the inhibitors in each of the minimum energy structures were evaluated using Clus-Pro online software.[46,47] The side chains of protein residues that interact with a given ligand are shown. Residues involved in interactions within ≤4.5 Å have only been shown.

molecules of these BPEs bind to the two hormone-binding pockets in an antiparallel orientation. In case of $R_1 = H$, the unsubstituted ring binds to P3 pocket and R_2 and R_3 substituted ring binds to the outer pocket to stabilize the structure (Figure 5). In the case of compounds **11** and **12**, the benzene ring binds deep in the P3 pocket making hydrophobic interactions, while heteroatoms N and O of the other ring are involved mainly in salt bridges with the residues lining the P1 pocket (Figure 5).

Fibril Disruption. The strong affinity of these compounds for TTR and the remarkable stability of the resulting complex prompted us to investigate their ability to inhibit TTR fibril elongation. Their ability to disrupt preformed fibers was also examined. BPEs examined were not only able to inhibit the elongation of early fibrils but also exhibited disruption of the mature fibrils in a dose-dependent manner. Moreover, these compounds also disrupted the formation of various intermediates
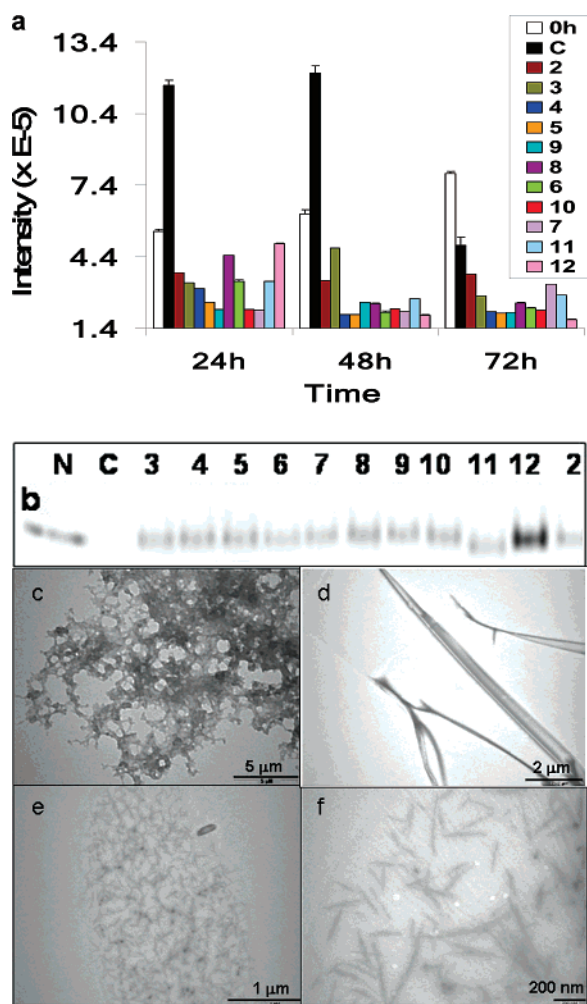
Figure 6. a: Th-T fluorescence of TTR fibers after disruption by compounds **2−12**. The TTR fiber formed at 24, 48, and 72 h were incubated with three doses (7.2 μM each) of compounds **2−12** for 15 days. The disruptions of preformed TTR fiber by these compounds were monitored by Th-T fluorescence by incubating samples with 50 μM of Th-T for 15 min at 37 °C. The samples were excited at 450 nm, and emissions were monitored at 480 nm. Results are mean of three different experiments executed in duplicates. b: Native-PAGE analysis of samples of TTR fibers disruption after 1 month of incubation with compounds **2−12** at 37 °C. TTR fibers incubated with compounds **2−12** for 15 days were centrifuged, and supernatant was loaded on gel to see the amount of soluble protein present. c−f: Transmission electron micrograph of control sample showing fibrillar aggregates (1:2 diluted, 4.2 K) (c), control sample showing full length fibers (1:100 diluted, 8.2 K) (d), fibers incubated with compounds **2−12** for 2 days were clearly disrupted (16.5 K) (e), magnified view of disrupted fibers (87 K) (f).

formed during TTR fibrilization. While single doses of inhibitors were adequate to prevent fibril elongation, multiple doses were required for the disruption of the preformed fibers. Disruption started after the second dose. The change in turbidity with time in the presence and the absence of compounds **2−12** is shown in Figure S4 (see Supporting Information). The disruption of fibrils formed at 24, 48, and 72 h, viz after three dosages of these compounds, was also confirmed by Th-T fluorescence assay (Figure 6a). While the fluorescence intensity of Th-T in control samples increased with time, no enhancement in intensity was observed in the samples incubated for 15 days with compounds **2−12**. All these compounds disrupt preformed TTR fibers as well. Compounds **4**, **5**, **6**, **9**, **10**, and **12** were found more effective as fibril disrupters under the conditions used.

Native-PAGE analysis of supernatants of above samples after 1 month clearly shows presence of abundant soluble protein compared to the untreated control (Figure 6b). Further, the effect of the compounds **2−12** on the ultrastructural properties of the TTR fiber was examined by TEM. Figure 6d shows the presence of abundant fibers (8−20 nm wide and 200−600 μm long) and fibrillar aggregates as compared to the control samples (Figure 6c). The fibrils with width of 14.4−21.6 μM were disrupted into fragments of 2−5 nm width and 20−100 μm long after the second dose of compounds **2−12**. Figure 6e and 6f shows a representative picture of the fibers disrupted by compounds **2−12** subsequent to their second and third doses, respectively.

Discussion

There is much evidence to show that conformational changes are sufficient for the conversion of a number of normally soluble human proteins into amyloid fibrils, the hallmark of human amyloid diseases.[6] Presently, there is no general strategy for treating human amyloid diseases. The most promising approach includes stabilization of the native state of these proteins, which is best exemplified by TTR amyloidosis. The earlier reports have demonstrated that native state kinetic stabilization is a viable therapeutic approach to prevent TTR amyloidosis.[45] In this study, we systematically screened a chemical library of 100 compounds and used structure-based design of substituted BPEs to construct small molecule inhibitors against TTR-associated amyloidosis. The site of amyloidosis *in vivo* in humans is not known. Therefore, we have evaluated these small molecule-based inhibitors of TTR amyloidosis under different conditions to demonstrate kinetic stabilization independent of experimental conditions. T4, a known inhibitor and natural ligand of TTR, was used for comparison in these screening studies. Screening of a chemical library and biphenyl ether derivatives, described in this report, yielded some of the most potent inhibitors of acid-mediated TTR fibril formation (see Table S1 in Supporting Information).

The experimental results (Figures 1−6 and Table 1) demonstrate that several biphenyl ether derivatives are excellent inhibitors of TTR (7.2 μM) fibril formation. Most of them have shown ∼ 100% inhibition of amyloidosis at 21.6 μM concentration when tested against 7.2 μM of TTR. The entire structure of **2**, **3**, and **6** appears to be important for their efficacy. Correlation of their structure with activity show that the $R_1 =$ Cl substituted phenyl ring is essential for inhibition as can be discerned from the poor activity of $R_1 = NO_2$ substituted BPE (Table S2 in Supporting Information). Compound **10**, an analogue of **2**, lacking both chlorine atoms, is less effective, indicating the importance of van der Waals interactions for their binding to TTR, a prerequisite for tetramer stabilization. Substitution at $R_2 =$ OH by OCH_3 in compound **7** decreases the activity. In contrast, activity was increased in compound **6**, indicating that substitution at R_3 position is valuable. Indeed, inhibitors **2**, **3**, and **6**, which are analogues of triclosan, also exhibited high potency signifying that carbonyl, carboxylic, and alkyl halide substitutions at R_3 position improve their efficacy over triclosan. Thus, the Cl group at the R_1 position and the carbonyl group at the R_3 position of these biphenyl derivatives are important for inhibition of TTR fibrillation. The number of active R_2- and R_3-substituted BPEs (**2-7**, Table 1) suggest that additional manipulation of BPE at these positions could yield inhibitors that are even more potent.

Of the 100 compounds from the chemical library, 41 compounds inhibited the process. Of these, two compounds (**11** and **12**) were found to be the most potent. The compounds thus

identified from the chemical library are heterocyclic compounds. The high potency and the significant differences in their molecular scaffolds as compared to the existing core structures (biphenyl ether, biphenyl amine, biphenyl, etc.), makes them promising leads for the design of potent TTR-specific amyloidosis inhibitors. Fibrillization of TTR with added compounds **1**−**12** buffered at pH 4.4 was similar, suggesting the affinity of inhibitors for TTR is greater than the propensity of TTR tetramer dissociation and misfolding. The IC_{50} determined for compounds **2**, **3**, and **6** are lowest values observed so far for the inhibition of TTR fibrillization. The low IC_{50} values (less than 1 equiv of TTR) for all these ligands clearly indicate that substantial inhibition of amyloidogenesis does not require kinetic stabilization of every TTR tetramer by the binding of a small molecule. Misfolded monomeric TTR aggregates into amyloid fibrils via a straightforward self-association mechanism where all forward steps in the pathway are favorable, whereas the rate of aggregation is dependent on the concentration of the misfolded TTR monomer.[46] Since the concentration of monomer depends on dissociation of the tetramer, controlling the energetics of tetramer dissociation will allow significant control over the amyloidogenic monomer concentration dictating the rate of TTR amyloidogenesis. Thus, tight binding of a small inhibitory molecule at substoichiometric concentrations (less than 1 equiv) may be sufficient to reduce the concentration of amyloidogenic monomeric TTR in the serum, thereby preventing the disease. This was evident by the kinetics of fibril formation in the presence and absence of inhibitors. A significant decrease in the rate of fibril formation by compounds **2**−**12** compared to the control was observed. The time course of TTR fibrillogenesis shows that it lacks a lag phase and is not seedable, which is in agreement with earlier reports.[47,45]

The dissociation constant for all these compounds at pH 4.4 correlates well with their efficacy. The strong negatively cooperative binding of compounds **2**, **3**, **4**, **6**, and **10** suggests that the binding of ligand to one site is sufficient to stabilize the tetramer to prevent amyloidosis. K_ds are low enough in case of **7**, **9**, **11**, and **12** to saturate both binding sites in TTR at 3.6 μM, i.e., equivalent to the physiological concentration (3.6 μM), ensuring that there is enough inhibitor to saturate both the binding sites. These biphenyl ether derivatives are better inhibitors as compared to T4 at lower concentrations. The inhibition of fibrillogenesis by compounds were further evaluated by Congo red binding and Thioflavin-T fluorescence (Figure 2a and 2c), as both bind specifically with protein fibers. Significant decrease in the amount of Congo red binding in the presence of inhibitors indicates absence of fibril formation compared to the unligated TTR. Similarly, binding of Th-T to TTR fibril and thus fluorescence was also decreased in the presence of compounds **1**−**12**, providing further support to our explanation about the inhibition of TTR amyloidosis by these compounds.

To understand the conformational states of the TTR in the presence and absence of inhibitors, intrinsic tryptophan fluorescence of the protein was monitored. Reduction in intensity at pH 7.2 in the presence of compounds **1**−**12** indicates interaction of these compounds leading to conformational change in protein (Figure 3a). In contrast, drastic reduction in the intensity was observed in TTR at pH 4.4 (Figure 3b). The emission maxima of TTR under fibrilogenesis conditions (pH 4.4) showed 3 nm red shift (343 nm) compared to TTR at pH 7.2, where emission maxima was at 340 nm, signifying a subtle conformational change at pH 4.4. In the presence of inhibitors, however, decreased quenching of TTR fluorescence was

observed under denaturing conditions, implying pH-independent stabilization of the protein in the presence of compounds **1**−**12**.

It has been reported earlier that the dissociation of the tetramer is a critical and rate-determining step in TTR related fibrillogenesis.[48] The ability of these inhibitors to impose kinetic stability on tetrameric TTR can be best evaluated by the rate of tetramer dissociation. Tetramer dissociation leads to the unfolding of the monomer in the presence of 6.0 M urea at 25 °C. To understand the mechanism of inhibition of fibril formation, denaturation kinetics of TTR in 6.0 M urea was carried out. The TTR tetramer does not denature in urea; however, dissociation to monomer is required for urea-induced tertiary structural changes which can be detected by monitoring the changes in intrinsic tryptophan fluorescence.[49,17] The TTR tetramer dissociation is drastically slowed down in the presence of compounds **1**−**12**, compared to the control. However, the decrease was less for T4 and triclosan, clearly indicating that the efficacies of the compounds **2**−**12** in increasing the energy barrier for tetramer dissociation is responsible for the stabilization of the tetramer of TTR.

Several reports indicate that inhibition of fibril formation can lead to accumulation of soluble prefibrillar oligomeric intermediates, the most cytotoxic species.[50,51] In the present study, cross-linking experiments with glutaraldehyde clearly show that even under the conditions conducive for fibrillization, TTR exists mostly as a tetramer in the presence of compounds **1**−**12** and T4 (Figure 4a). In contrast, no tetramer was observed in unligated TTR, ruling out the possibility of the formation of the prefibrillar cytotoxic species in the presence of compounds **2**−**12** during fibril formation. The stability of TTR−inhibitor complex was determined under denaturing condition by extending the incubation time to 7−15 days. An analysis of MALDI-TOF data shows remarkable stability of TTR by BPEs compared to that observed in the presence of T4 (Figure 4b). Even after 30 days of incubation, TTR retains its tetrameric structure in the presence of 3 equiv of compounds **2**−**12** under conditions, in which the absence of these compounds would have led to fibrilization within 72 h.

An increasing appreciation of soluble oligomeric intermediate as the major cytotoxic species in amyloidosis prompted us to test the effect of these compounds on TTR-induced cytotoxicity in Neuro2A cells. The cell cytotoxicity assay shows that TTR-induced cytotoxicity was inhibited by the compounds **2**−**12** that stabilize the TTR tetramer (Figure 4c). Interestingly, these inhibitors are not cytotoxic at the concentration tested and add to the potential of these BPEs as inhibitors of fibril formation and the consequent pathogenesis of the disease.

An analysis of TTR−ligand docking studies indicates that the BPEs establish optimum interactions within the hormone binding site (Figure 5). Binding of BPEs to TTR are dominated by hydrophobic and electrostatic interactions with residues 15, 17, 108, 110, 117, 119, and 121. In spite of their common structural features, considerable differences were observed in the mode of binding to the T4 binding site. While the halogen binding pockets in TTR provide primarily a hydrophobic surface, conformational changes of its side chains facilitate additional hydrogen bonding interactions. The ligand-induced conformational changes of TTR not only allow energetically favorable interactions between ligand and the protein but also stabilize the nonamyloidogenic tetramer of TTR against pH-mediated dissociation by the formation of inter-subunit hydrogen bonds.

Besides, inhibiting the fibril formation, these compounds are also able to prevent the elongation of small prefibrillar species

(Figure 6). Fibril formation is completed within 72−80 h in case of TTR, and compounds **2**−**12** disrupt the fibers within this time limit, signifying the presence of structural motifs for the binding of these compounds.

Conclusion

The results presented above establish that the biphenyl ether template provides the shape and size complementarity to the TTR binding pocket, and carbonyl/carboxylic and chloride groups at position R_3 and R_1, respectively, are necessary for potentiating the interactions. The high potency of some of these compounds compared to any of the inhibitors described so far can be explained by their structural complementarity to the T4 binding region of TTR as well as the solubility and stability of the complexes. Moreover, binding of compounds **2**−**12** has an overall stabilizing effect on the TTR quaternary structure that surpasses the ability of other inhibitors. These molecules are able to prevent cytotoxicity induced by TTR in a neuronal cell culture. Further, they inhibit the fibril elongation at any step of the process as well as disrupt the preformed fibrils. The present study also shows that compounds **11** and **12** could be promising new structural templates for the design of potent inhibitors as therapeutic agents against TTR amyloidosis.

All of the compounds studied here act by raising the energy barrier for dissociation by stabilizing the tetrameric ground state of TTR. The kinetic stabilization of the TTR tetramer is the most feasible strategy, since the identity of the species of the TTR amyloidogenesis pathway that induces toxicity still remains unknown. Although binding of these compounds to any amyloidogenic TTR mutants has not been tested, there are reports showing little or no structural changes in tetrameric conformation and T4 binding site in most of the TTR mutants. Hence, it can be assumed that molecules, which bind to wild type TTR, may also bind to these mutants. Therefore, a therapeutic strategy based on the development and administration of small molecules inhibitors could be explored for the prophylaxis of asymptomatic gene carriers. TTR has been shown to play an important role in keeping Aβ in soluble form.[8] Hence, the increased stabilization of TTR by these compounds might also prevent the progression of other neurodegenerative disorders.

Experimental Section

Preparation of Inhibitors. The chemical library was purchased from Chemical Diversity Labs Inc, San Diego, CA. Synthesis of substituted BPE has recently been reported by our group.[52] Triclosan was obtained from Kumar Chemicals, Bangalore, India. The schemes used for the synthesis of the BPEs are provided in the Supporting Information. Stock solutions (10 mM) of the compounds used were prepared in DMSO. All compounds diluted from the stock solution were soluble at 50−100 μm concentrations in aqueous buffer used for assessing their inhibitory potencies in assays to monitor TTR amyloidosis.

Expression and Purification of WT-TTR. TTR cloned in pMMHa vector was a kind gift of Dr. P. Raghu from National Institute of Nutrition, Hyderabad, India. Protein expression and purification was performed as reported earlier.[53] Protein concentrations were measured by absorbane at 280 nm. Protein purity was assessed by SDS-PAGE, and its mass was confirmed by electrospray ionization mass spectrometry (ESI-MS).

Stagnant Acid-Mediated TTR Aggregation Assay. The efficacy of compounds **1**−**12** was determined by stagnant acid-mediated turbidity assay at 340 nm using Tecan GENios microplate reader. Details of the assay are provided as Supporting Information. The solution of TTR tetramer (7.2 μM; 0.4 mg/mL) in 5 mM sodium phosphate, 100 mM KCl, 1 mM EDTA, pH 7, were incubated with inhibitor at 7.2 and 21.6 μM, viz, TTR tetramer to

inhibitor ratio of 1:1 and 1:3, respectively, in 1% DMSO in a total volume of 0.5 mL. The experiments were conducted at 25 °C. After 1 h, the samples were diluted with 0.5 mL of 200 mM sodium acetate buffer pH 4.4 containing 100 mM KCl and 1 mM EDTA, vortexed, and incubated at 37 °C for 72 h. In another assay, inhibitors were buffered in the same pH 4.4 buffer, and TTR was added directly to this solution and incubated at 37 °C for 72 h to assess the affinity of these inhibitors for TTR under fibrillation condition. The IC$_{50}$ of inhibition of these inhibitors were studied by incubating the TTR (7.2 μM) with 0.5−50 μM of inhibitors, and the IC$_{50}$ values were calculated graphically as provided in Supporting Information. The stoichiometry of the binding of the inhibitors was determined by HPLC as described by Green et al.,[23] Dissociation constant of binding of these compounds to TTR was determined by fluorescence titration, and data were fitted into the Adair equation for two binding sites as given in Supporting Information. All experiments were done in triplicate.

Time Course of Fibril Formation. The kinetics of inhibition was studied by taking 7.2 μM TTR and 21.6 μM of inhibitors in a 96-microwell plate. The change in turbidity was monitored at 340 nm in the microplate reader using Magellan software. Details are given in Supporting Information. All experiments were performed three times in triplicates. Change in absorbance (mean of three different experiments) at 340 nm was plotted against time in the presence and absence of inhibitors. Initial rate of fibril formation was calculated from the value of the slope by linear fitting of the change in absorbance at 340 nm as a function of time.

Congo Red Binding. The amount of bound Congo red was estimated as reported earlier[53] using the equation, moles of Congo red bound/L of amyloid suspension = A_{540}(nm)/25295 − A_{477}(nm)/46306.

Thioflavin-T Fluorescence. The thioflavin-T (ThT) binding assays were performed in a Jobin Yvon Fluoromax spectrofluorimeter using an excitation slit width of 2 nm and emission slit width of 5 nm as reported earlier.[55] In brief, samples were incubated with 50 μM of Th-T for 15 min at 37 °C in the dark. The samples were excited at 450 nm, and emissions were monitored at 480 nm. The inner filter effect was corrected by using the following equation,

$$F_c = F \times \text{antilog}[(A_{ex} + A_{em})/2]$$

where F_c is the corrected fluorescence and F is the measured one, A_{ex} and A_{em} are the absorbances of the reaction solution at the excitation and emission wavelengths, respectively. All experiments were done in triplicate.

Intrinsic Fluorescence of TTR. For monitoring the intrinsic fluorescence of TTR, 0.2 mL of 3.6 μM TTR solutions was incubated with 10.8 μM concentration of a given inhibitor at pH 7.2 and 4.4. Samples were excited at 290 nm, and emission was recorded between 310 and 370 nm. All the experiments were performed at least three times and typically in duplicates.

Urea Denaturation. TTR (1.8 μM) was incubated with 5.4 μM inhibitors at 37 °C for 30 min in 400 μL of 50 mM phosphate buffer containing 1 mM EDTA, 1 mM DTT and 100 mM KCl. After 30 min, 600 μL of 10 M urea stock in the same buffer was added to bring the final concentration of urea to 6 M. Tryptophan fluorescence was measured in the range of 310−370 nm up to 144 h as described above and corrected for inner filter effect. The results are the mean of three different experiments done in duplicates.

Glutaraldehyde Cross-Linking. The quaternary structural changes of TTR at pH 4.4 in the presence and absence of all these inhibitors was monitored by glutaraldehyde cross-linking and SDS−PAGE.[56] The cross-linked samples were run on 12.5% SDS−PAGE. TTR incubated at pH 7.5 was used as a control. The gels were stained with Coomassie brilliant blue and analyzed by Bio-Rad GS-710 imaging densitometer.

Mass Spectrometry. Aliquots of the samples of TTR kept for assaying fibril formation in the absence (0 h sample) and presence of compounds **1**−**12** at 3−15 days were centrifuged at 15 000 rpm for 30 min and then filtered through 80 kDa cutt-off membranes. Subsequently, 1 μL of the filtrate was mixed with 1 μL of matrix,

3-(4-hydroxy-3,5-dimethoxy-phenyl)prop-2-enoic acid in ethanol containing 0.5% trifluoroacetic acid and loaded on to the target plate. Mass spectra were recorded using Brucker MALDI-TOF instrument. TTR frozen at -20 °C, pH 7.4, was used as the positive control.

Cell Culture and Cytotoxicity Inhibition Assay. The effect of TTR and compounds **2**−**12** on adherent human neuro2a cell line was monitored as described earlier.[57] Experimental details are provided in the Supporting Information. All the assays were carried out twice in triplicates. The results were calculated as (% viability)/(% cytotoxicity).

Molecular Docking. The MOE-2005 (Molecular Operating Environment) software was used to perform docking. The inbuilt algorithms were followed. Before docking, the coordinates of the biphenyl ethers were energy minimized using the force field MMFF94. Prior to docking studies all the water molecules have been removed from TTR (PDB code 1e4h) structure. Molecular docking with the TTR tetramer was done with each of the mentioned compounds. From a cluster of 100 docked structures, the one with the minimum energy was considered for further studies. Further, we evaluated the interactions between TTR and the inhibitors in each of the minimum energy structures using LPC-CSU online software.[58] We overlapped these docked structures of compounds **1**−**12** with the crystal structure of T4 bound to human TTR (PDB code 2ROX) to validate the accuracy of docking experiments.

Fibril Disruption Assay. A 14.4 μM concentration of TTR was incubated with 100 mM sodium acetate pH 4.4 containing 1 mM EDTA, 0.1M KCl for 0, 1 3, 6, 12, 24, 48, and 72 h at 37 °C. After indicated time points, the fibers (7.2 μM) were incubated with the compounds **2**−**12** (14.4 μM) in PBS at 37 °C. The disruption was followed for 7 days by turbidity measurements at 340 nm and Th-T fluorescence. A second dose of the inhibitor (7.2 μM) was added after 24 h of incubation, and samples were incubated and monitored further for 5−6 days. After 15−20 days of incubation, samples were examined by transmission electron microscopy (TEM). All experiments were done thrice in triplicates each time.

Transmission Electron Microscopy. The samples were vortexed and immediately absorbed to glow discharged carbon-coated 200 mesh copper grids. Negative staining was done by 3% uranyl acetate. Details of the method used are given in the Supporting Information. The grids were visualized with a FEI TECNAI G2 at 120 kV. The picture was captured using Mega View III camera and analyzed using AnalySIS Software from Imaging System GmbH.

Supporting Information Available: The experimental section, schemes of biphenyl ethers synthesis, TEM showing different fibril morphologies, mass spectra of TTR inhibitor complexes, inhibition of fibril elongation and fibril disruption (turbidity assay). Tables containing results of all the compounds tested and purity data of synthesized compounds. This material is available free of charge via the Internet at http://pubs.acs.org.

References

(1) Kisilevsky, R. Amyloid beta threads in the fabric of Alzheimer's disease. *Nat. Med.* **1999**, *4*, 772−773.

(2) Harrison, P. M.; Bamborough, P.; Daggett, V.; Prusiner, S. B.; Cohen, F. E. The prion folding problem. *Curr. Opin. Struct. Biol.* **1997**, *7*, 53−59.

(3) Reese, W.; Hopkovitz, A.; Lifschitz, M. D. B2-microglobulin and associated amyloidosis presenting as bilateral popliteal tumors. *Am. J. Kidney Dis.* **1988**, *12* (4), 323−325.

(4) Kelly, J. W. Amyloid fibril formation and protein misassembly: a structural quest for insights into amyloid and prion diseases. *Structure* **1997**, *5*, 595−600.

(5) Westermark, P.; Wernstedt, C.; Wilander, E.; Hayden, D. W.; O'Brien, T. D.; Johnson, K. H. Amyloid fibrils in human insulinoma and islets of Langerhans of the diabetic cat are derived from a neuropeptide-like protein also present in normal islet cells. *Proc. Natl. Acad. Sci. U.S.A.* **1987**, *84*, 3881−3885.

(6) Dabson, C. M. Protein misfolding, evolution and disease. *Trends Biochem. Sci.* **1999**, *9*, 329−332.

(7) Hamilton, J. A.; Benson, M. D. Protein misfolding, evolution and disease. *Cell Mol. Life Sci.* **2000**, *58*, 1491−1521.

(8) Lin Liu Murphy, R. M. Kinetics of Inhibition of β-Amyloid Aggregation by Transthyretin. *Biochemistry* **2006**, *45*, 15702−15709.

(9) Gustavsson, A.; Jahr, H.; Tobiassen, R.; Jacobson, D. R.; Sletten, K.; Westermark, P. Amyloid fibril composition and transthyretin gene structure in senile systemic amyloidosis. *Lab. Invest.* **1995** *73* (5), 703−708.

(10) Saraiva, M. J. Transthyretin mutations in health and disease. *Hum. Mutat.* **1995**, *5* (3), 191−196.

(11) Vidal, R.; Garzuly, F.; Budka, H.; Lalowski, M.; Linke, R. P.; Brittig, F.; Frangione, B.; Wisniewski, T. Meningocerebrovascular amyloidosis associated with a novel transthyretin mis-sense mutation at codon 18 (TTRD 18G). *Am. J. Pathol.* **1996**, *148*, 361−366.

(12) Hammarström, P.; Sekijima, Y.; White, J. P.; Wiseman, R. L.; Lim, A.; Costello, C. E.; Altland, K.; Garzuly, F.; Budka, H.; Kelly, J. W. D18G transthyretin is monomeric, aggregation prone, and not detectable in plasma and cerebrospinal fluid: a prescription for central nervous system amyloidosis? *Biochemistry* **2003**, *42*, 6656−6663.

(13) Quintas, A.; Saraiva, M. J.; Brito, R. M. M. The tetrameric protein transthyretin dissociates to a non-native monomer in solution. A novel model for amyloidogenesis. *J. Biol. Chem.* **1999**, *274*, 32943−32949.

(14) Jacobson, D. R.; Pastore, R. D.; Yaghoubian, R.; Kane, I.; Gallo, G.; Buck, F. S.; Buxbaum, J. N. Variant-sequence transthyretin (isoleucine 122) in late-onset cardiac amyloidosis in black Americans. *N. Engl. J. Med.* **1997**, *336*, 466−473.

(15) Blake, C. C.; Geisow, M. J.; Oatley, S. J.; Rerat, B.; Rerat, C. F. Structure of prealbumin: secondary, tertiary and quaternary interactions determined by Fourier refinement at 1.8 A. *J. Mol. Biol.* **1978**, *121*, 339−356.

(16) Bartalena, L.; Robbins, J. Thyroid hormone transport proteins. *Clin. Lab. Med.* **1993**, *13*, 583−598.

(17) Hammarström, P.; Schneider, F.; Kelly, J. W. Trans-suppression of misfolding in an amyloid disease. *Science* **2001**, *293*, 2459.

(18) Hammarstrom, P.; Wiseman, R. L.; Powers, E. T.; Kelly, J. W. Prevention of transthyretin amyloid disease by changing protein misfolding energetics. *Science* **2003**, *299*, 713−716.

(19) Morais-de-Sa, E.; Neto-Silva, R. M.; Pereira, P. J.; Saraiva, M. J.; Damas, A. M. The binding of 2,4-dinitrophenol to wild-type and amyloidogenic transthyretin. *Acta Crystallogr. D Biol. Crystallogr.* **2006**, *62* (5), 512−519.

(20) Morais-de-Sa, E.; Pereira, P. J.; Saraiva, M. J.; Damas, A. M. The crystal structure of transthyretin in complex with diethylstilbestrol: a promising template for the design of amyloid inhibitors. *J. Biol. Chem.,* **2004**, *279*, 53483−53490.

(21) Gales, L.; Macedo-Ribeiro, S.; Arsequell, G.; Valencia, G.; Saraiva, M. J.; Damas, A. M. Human transthyretin in complex with iododiflunisal: structural features associated with a potent amyloid inhibitor. *Biochem. J.* **2005**, *388*, 615−621.

(22) Green, N. S.; Foss, T. R.; Kelly, J. W. Genistein, a natural product from soy, is a potent inhibitor of transthyretin amyloidosis. *Proc. Natl. Acad. Sci. U.S.A.* **2005**, *102*, 14545−14550.

(23) Green, N. S.; Palaninathan, S. K.; Sacchettini, J. C.; Kelly, J. W. Synthesis and characterization of potent bivalent amyloidosis inhibitors that bind prior to transthyretin tetramerization. *J. Am. Chem. Soc.* **2003**, *125*, 13404−13414.

(24) Johnson, S. M.; Petrassi, H. M.; Palaninathan, S. K.; Mohamedmohaideen, N. N.; Purkey, H. E.; Nichols, C.; Chiang, K. P.; Walkup, T.; Sacchettini, J. C.; Sharpless, K. B.; Kelly, J. W. Bisaryloxime ethers as potent inhibitors of transthyretin amyloid fibril formation. *J. Med. Chem.* **2005**, *48*, 1576−1587.

(25) Petrassi, H. M.; Johnson, S. M.; Purkey, H. E.; Chiang, K. P.; Walkup, T.; Jiang, X.; Powers, E. T.; Kelly, J. W. Potent and selective structure-based dibenzofuran inhibitors of transthyretin amyloidogenesis: kinetic stabilization of the native state. *J. Am. Chem. Soc.* **2005**, *127*, 6662−6671.

(26) Petrassi, H. M.; Klabunde, T.; Sacchettini, J.; Kelly, J. W. Structure-Based Design of N-Phenyl Phenoxazine Transthyretin Amyloid Fibril Inhibitors. *J. Am. Chem. Soc.* **2000**, *122*, 2178−2192.

(27) Adamski-Werner, S. L.; Palaninathan, S. K.; Sacchettini, J. C.; Kelly, J. W. Diflunisal analogues stabilize the native state of transthyretin. Potent inhibition of amyloidogenesis. *J. Med. Chem.* **2004**, *47*, 355−374.

(28) Almeida, M. R.; Macedo, B.; Cardoso, I.; Alves, I.; Valencia, G.; Arsequell, G.; Planas, A.; Saraiva, M. J. Selective binding to transthyretin and tetramer stabilization in serum from patients with familial amyloidotic polyneuropathy by an iodinated diflunisal derivative. *Biochem. J.* **2004**, *381*, 351−356.

(29) Miller, S. R.; Sekijima, Y.; Kelly, J. W. Native state stabilization by NSAIDs inhibits transthyretin amyloidogenesis from the most common familial disease variants. *Lab. Invest.* **2004**, *84*, 545−552.

(30) Razavi, H.; Palaninathan, K, S.; Powers, E. T.; Wiseman, R. L.; Purkey, H. E.; Mohamedmohaideen, N. N.; Deechonkit, S.; Chiang, K. P.; Dendle, M. T. A.; Sacchettini, J. C.; Kelly, J. W. Benzoxazoles as transthyretin amyloid fibril inhibitors: synthesis, evaluation, and mechanism of action. *Angew. Chem.* **2003**, *42*, 2758−2761.

(31) Cardoso, I.; Merlini, G.; Saraiva, M. J. 4′-iodo-4′-deoxydoxorubicin and tetracyclines disrupt transthyretin amyloid fibrils in vitro producing noncytotoxic species: screening for TTR fibril disrupters. *FASEB J.* **2003**, *17*, 803−809.

(32) Sebastiao, M. P.; Merlini, G.; Saraiva, M. J.; Damas, A. M. The molecular interaction of 4′-iodo-4′-deoxydoxorubicin with Leu-55Pro transthyretin 'amyloid-like' oligomer leading to disaggregation. *Biochem. J.* **2000**, *351*, 273−279.

(33) Oza, V. B.; Smith, C.; Raman, P.; Koepf, E. K.; Lashuel, H. A.; Petrassi, H. M.; Chiang, K. P.; Powers, E. T.; Sacchettini, J.; Kelly, J. W. S. Synthesis, structure, and activity of diclofenac analogues as transthyretin amyloid fibril formation inhibitors. *J. Med. Chem.* **2002**, *45*, 321−332.

(34) Raghu, P.; Reddy, G. B.; Sivakumar, B. Inhibition of transthyretin amyloid fibril formation by 2,4-dinitrophenol through tetramer stabilization. *Arch. Biochem. Biophys.* **2002**, *400* (1), 43−47.

(35) Klabunde, T.; Petrassi, H. M.; Oza, V. B.; Raman, P.; Kelly, J. W.; Sacchettini, J. C. Rational design of potent human transthyretin amyloid disease inhibitors. *Nat. Struct. Biol.* **2000**, *7*, 312−321.

(36) Peterson, S. A.; Klabunde, T.; Lashuel, H.; Purkey, H.; Sacchettini, J. C.; Kelly, J. W. Inhibiting transthyretin conformational changes that lead to amyloid fibril formation. *Proc Natl Acad Sci U.S.A.* **1998**, *95*, 12956−12960.

(37) Baures, P. W.; Peterson, S. A.; Kelly, J. W. Discovering transthyretin amyloid fibril inhibitors by limited screening. *Bioorg. Med. Chem.* **1998**, *6*, 1389−1401.

(38) Miroy, G. J.; Lai, Z.; Lashuel, H. A.; Peterson, S. A.; Strang, C.; Kelly, J. W. Inhibiting transthyretin amyloid fibril formation via protein stabilization. *Proc. Natl. Acad. Sci. U.S.A.* **1996**, *93*, 15051−15056.

(39) Erlanson, D. A.; Hansen, S. K. Making drugs on proteins: site-directed ligand discovery for fragment-based lead assembly. *Curr. Opin. Chem. Biol.* **2004**, *8*, 399−406.

(40) Altland, K.; Winter, P.; Saraiva, M. J.; Suhr, O. Sulfite and base for the treatment of familial amyloidotic polyneuropathy: two additive approaches to stabilize the conformation of human amyloidogenic transthyretin. *Neurogenetics* **2004**, *5*, 61−67.

(41) Altland, K.; Winter, P. Potential treatment of transthyretin-type amyloidoses by sulfite. *Neurogenetics* **1999**, *2*, 183−188.

(42) Dolado, I.; Nieto, J.; Saraiva, M. J.; Arsequell, G.; Valencia, G.; Planas, A. Kinetic assay for high-throughput screening of in vitro transthyretin amyloid fibrillogenesis inhibitors. *J. Comb. Chem.* **2005**, *7*, 246−252.

(43) Surolia, N.; Surolia, A. Triclosan offers protection against blood stages of malaria by inhibiting enoyl-ACP reductase of Plasmodium falciparum. *Nat. Med.* **2001**, *7*, 167−173.

(44) Wojtczak, A.; Cody, V.; Luft, J. R.; Pangborn, W. Structures of human transthyretin complexed with thyroxine at 2.0 A resolution and 3′,5′-dinitro-N-acetyl-L-thyronine at 2.2 A resolution. *Acta Crystallogr., Sect. D: Biol. Crystallogr.* **1996**, *52*, 758−765.

(45) Weisman, L. R.; Johnson, S. M.; Kelker, M. S.; Foss, T.; Wilson, I. A.; Kelly, J. W. Kinetic stabilization of an oligomeric protein by a single ligand binding event. *J. Am. Chem. Soc.*, **2005**, *127*, 5540−5551.

(46) Hurshman, A. R.; White, J. T.; Powers, E. T.; Kelly, J. W. Transthyretin aggregation under partially denaturing conditions is a downhill polymerization. *Biochemistry* **2004**, *43*, 7365−7381.

(47) White, J. T.; Kelly, J. W. Support for the multigenic hypothesis of amyloidosis: the binding stoichiometry of retinol-binding protein, vitamin A, and thyroid hormone influences transthyretin amyloidogenicity in vitro. *Proc. Natl. Acad. Sci. U.S.A.* **2001**, *98*, 3019−3024.

(48) Jiang, X.; Buxbaum, J. N.; Kelly, J. W. The V122I cardiomyopathy variant of transthyretin increases the velocity of rate-limiting tetramer dissociation, resulting in accelerated amyloidosis. *Proc. Natl. Acad. Sci. U.S.A.* **2001**, *98*, 14943−14948.

(49) Hammarstrom, P.; Jiang, X.; Hurshman, A. R.; Powers, E. T.; Kelly, J. W. Sequence-dependent denaturation energetics: A major determinant in amyloid disease diversity. *Proc. Natl. Acad. Sci. U.S.A.* **2002**, *99*, 16427−16432.

(50) Reixach, N.; Deechongkit, S.; Jiang, X.; Kelly, J. W.; Buxbaum, J. N. Tissue damage in the amyloidoses: Transthyretin monomers and nonnative oligomers are the major cytotoxic species in tissue culture. *Proc. Natl. Acad. Sci. U.S.A.* **2004**, *101*, 2817−2822.

(51) Sousa, M. M.; Cardoso, I.; Fernandes, R.; Guimaraes, A.; Saraiva, M. Deposition of transthyretin in early stages of familial amyloidotic polyneuropathy: evidence for toxicity of nonfibrillar aggregates. *J. Am. J. Pathol.* **2001**, *159*, 1993−2000.

(52) Chhibber, M.; Kumar, G.; Parasuraman, P.; Ramya, T. N.; Surolia, N.; Surolia, A. Novel diphenyl ethers: design, docking studies, synthesis and inhibition of enoyl ACP reductase of Plasmodium falciparum and Escherichia coli. *Bioorg. Med. Chem.* **2006**, *14* (23), 8086−8098.

(53) Lashuel, H. A.; Wurth, C.; Woo, L.; Kelly, J. W. The most pathogenic transthyretin variant, L55P, forms amyloid fibrils under acidic conditions and protofilaments under physiological conditions. *Biochemistry* **1999**, *38* (41), 13560−135revised73.

(54) Klunk, W. E.; Jacob, R. F.; Mason, R. P. Quantifying amyloid by Congo red spectral shift assay. *Methods Enzymol.* **1999**, *309*, 285−3005.

(55) Le Vine, H. Quantification of β-Sheet Amyloid Fibril Structures with Thioflavin T. *Methods Enzymol.* **1999**, *309*, 274−284.

(56) Colon, W.; Kelly, J. W. Partial denaturation of transthyretin is sufficient for amyloid fibril formation in vitro. *Biochemistry* **1992**, *31*, 8654−8660.

(57) Surolia, I.; Reddy, G. B.; Sinha, S. Hierarchy and the mechanism of fibril formation in ADan peptides. *J. Neurochem.* **2006**, *99*, 537−548.

(58) Sorokine, A.; Prilusky, J.; Abola, E. E.; Edelman, M. Automated analysis of interatomic contacts in proteins. *Bioinformatics* **1999**, *15*, 327−332.